JOURNAL OF MATERIALS SCIENCE 31 (1996) 749–755

Fracture toughness and crack morphology in indentation fracture of brittle materials

M. TANAKA
Department of Mechanical Engineering, Mining College, Akita University, 1-1, Tegatagakuen-cho, Akita 010, Japan

The relationship between the indentation fracture toughness, K_c, and the fractal dimension of the crack, D, has been examined on the indentation-fractured specimens of SiC and AlN ceramics, a soda–lime glass and a WC–8%Co hard metal. A theoretical analysis of the crack morphology based on a fractal geometry model was then made to correlate the fractal dimension of the crack, D, with the fracture toughness, K_{IC}, in brittle materials. The fractal dimension of the indentation crack, D, was found to be in the range 1.024–1.145 in brittle materials in this study. The indentation fracture toughness, K_c, increased with increasing fractal dimension, D, of the crack in these materials. According to the present analysis, the fracture toughness, K_{IC}, can be expressed as the following function of the fractal dimension of the crack, D, such that

$$\ln K_{IC} = 1/2\{\ln[2\Gamma E/(1-\nu^2)] - (D-1)\ln r_L\}$$

where Γ is the work done in creating a unit crack surface, E is Young's modulus, ν is Poisson's ratio, and r_L is r_{min}/r_{max}, the ratio of the lower limit, r_{min}, to the upper limit, r_{max}, of the scale length, r, between which the crack exhibits a fractal nature ($r_{min} \leqslant r \leqslant r_{max}$). The experimental data (except for WC–8%Co hard metal) obtained in this study and by other investigators have been fitted to the above equation. The factors which affect the prediction of the value of K_{IC} from the above equation have been discussed.

1. Introduction

Since Mandelbrot *et al.* [1] revealed a relationship between the absorbed energy and the fractal dimension of the fracture surface in the impact-loaded and fractured steels, the concept of the fractal geometry has been applied to problems in engineering materials [2–8]. Mecholsky *et al.* [9] and Milman *et al.* [10] studied fracture surfaces of alumina and glass-ceramics and fitted the relation of the fractal dimension of the fracture surface, $D'(1 \leqslant D' \leqslant 2)$, and the critical stress intensity factor, K_{IC}, with the form $K_{IC} = K_0 + Ea_0^{1/2}(D'-1)^{1/2}$, where K_0 is the value of K_{IC} for the hypothetical material with the smooth fracture surface, E is Young's modulus, and a_0 is a parameter that has units of length. This equation indicates that the increase of the fractal dimension of the fracture surface leads to the increase in the fracture toughness of the ceramic materials. From the engineering point of view, it is important to know the quantitative relationship between the crack morphology and the fracture toughness in brittle materials, because the crack deflection is one of the viable toughening mechanisms in brittle materials [11, 12].

The microstructures including dispersion of second-phase particles, grain–boundary configuration and grain size, generally affect the fractal dimension of fracture surfaces, the mechanical properties and the fracture mechanisms in metallic materials (6, 13–16), although the effect of each microstructure prevails in a limited scale range, depending on the characteristic dimension of the microstructure (5, 6, 15, 16). Even in ceramics, as well as ductile metallic materials, the strength and toughness of materials is largely influenced by microstructures of the materials [11, 12]. Thus, it is important to know what microstructure the measured fractal dimension of the cracks is associated with, because the crack morphology estimated by the fractal dimension of the crack can also be affected by the size of the microstructures in brittle materials.

Many experimental methods have been proposed for the estimation of the fracture toughness of ceramics [17, 18]. Among these, the indentation fracture (IF) method is known as the most convenient method and can estimate the fracture toughness of a small area in microstructures [17]. The indentation fracture toughness, K_c, is not exactly the plane-strain fracture toughness, K_{IC}, and there are many difficulties about the determination of indentation crack type (i.e. median crack or Palmqvist crack) and K_{IC} value in the IF method [19, 20], but there is a correlation between the K_C value and the K_{IC} value in brittle materials [17, 18].

0022–2461

In this study, the indentation fracture toughness, K_c, and the fractal dimension of the crack, D, were examined on indentation-fractured specimens of SiC and AlN ceramics, a soda–lime glass and a WC–8%Co hard metal. An analysis of the crack morphology was made on the basis of a fractal geometry model, and a theoretical equation was developed to correlate the fractal dimension of the crack, D, with the fracture toughness, K_{IC}, in brittle materials. The experimental results obtained in this study and by Mecholsky *et al.* [9] were then fitted to this equation. The factors which affect the prediction of the value of K_{IC} from the theoretical equation were also discussed. Further, the correlations between the scale length of the fractal analysis, the size of microstructures such as grain diameter and crack length, were also examined.

2. Experimental procedure

A silicon carbide (Norton NC-430 SiC), a hot-pressed aluminium nitride (HP-AlN), a WC–8%Co hard metal used in the previous study [21] and a commercial soda–lime glass, were used for the indentation fracture experiments and the estimation of the fractal dimension of the indentation crack. Table I shows the physical and mechanical properties of the materials used in this study. The specimens of these materials were supplied in the form of rectangular bars of 3 mm × 5 mm × 50 mm (HP-AlN) or 5 mm × 5 mm × 50 mm (WC–8%Co), or in the form of plates of 20 mm × 20 mm × 5 mm (soda–lime glass) or 10 mm × 20 mm × 5 mm (Norton NC-430 SiC). The soda–lime glass specimens were annealed for 1.8 ks at 693 K. All the specimens were mechanically polished with a diamond paste of 3 μm grain size and finished with a diamond paste of 0.25 μm grain size. The specimen of Norton NC-430 SiC was electrolytically etched in 20 g KOH–100 ml water solution, that of WC–8%Co was etched in 25 ml HNO_3–75 ml HCl solution, and the specimen of HP-AlN was etched in 10 ml acetic acid–10 ml HNO_3–10 ml water solution [24] before the indentation fracture experiments. Table II shows the average grain diameter or the average diameter of second-phase particles in the specimens of brittle materials. The average grain diameter of the specimens was estimated by Fullman's method [25].

The indentation fracture experiments were carried out using Vickers hardness testers under a load of 490 N (the specimen of WC–8%Co hard metal) or 9.8 N (other specimens). The indentation fracture toughness, K_c, value of the specimen was obtained as the one averaged over 10 datum points for WC–8%Co hard metal and as the value averaged over 5 datum points for other materials. The indentation crack observed in soda–lime glass was found to be "median crack" by using an optical microscope, while "Palmqvist crack" was known to occur in the indentation fracture of WC–8%Co hard metal [21]. According to Nishida and Yasuda [17] and Niihara *et al.* [18], the type of crack in the specimens of SiC and AlN ceramics were distinguished by examining the relationship between the indentation load and the crack length in the loading range from 0.98–9.8 N, because a direct observation of indentation cracks was not made in these materials. It was assumed from the experimental results that the median crack occurred in the indentation-fractured specimens of SiC and AlN ceramics. The indentation fracture toughness, K_c, was estimated from the following equation

$$K_c = 0.013(E/H)^{1/2}(P/c^{3/2}) = 0.02E^{0.5}P^{0.5}a^{-0.5}(c/a)^{-1.5} \quad (1)$$

for median cracks in low-toughness materials [17, 26], and from

$$K_c = 0.012(E/H)^{2/5}(HP/l)^{1/2} = 0.011E^{0.4}P^{0.6}a^{-0.7}(l/a)^{-0.5} \quad (2)$$

for Palmqvist cracks in high-toughness materials [17, 27], where c is the radius of median cracks, a is half of the diagonal length of indentation, H is the Vickers hardness ($H = 0.464P/a^2$), E is Young's modulus and l is the crack length ($l = c - a$).

The indentation cracks in specimens were observed with an optical microscope. Optical micrographs of the crack profiles were taken at the magnifications of × 50–× 1000 were used for the fractal analysis of the indentation crack. The coarse-graining method using line segments was employed in this study [28, 29]. The crack profile is approximated by line segments of the length r, as shown in Fig. 1. If N is the number of these line segments, the value of N is generally correlated

TABLE I The physical and mechanical properties of the materials used in this study

Material	Young's modulus E (GPa)	Fracture toughness K_{IC}(MPa m$^{1/2}$)	Density g cm^{-3}	Bending strength (MPa)
Norton NC-430 SiC	400[a]	3.5[a]	3.1[a]	310[a] (20°C)
HP–AlN	340[b]	–	3.3[b]	–
Soda–lime glass	68[b]	–	2.5[b]	–
WC–8%Cohard metal	590[c]	13.3[d]	–	–

[a] Data reported by the manufacturers.
[b] Data taken from [22].
[c] Young's modulus taken from [23].
[d] K_{IC} value obtained using SENB (single edge-notched bend) specimens in the previous study [21].

TABLE II The average grain diameter or the average diameter of second-phase particles in the specimens of brittle materials

Material	Average grain or particle diameter (grain or particle size range) (m)
Norton NC-430 SiC	1.3×10^{-5} (3.7×10^{-7} to 8.6×10^{-5}
HP–AlN	6.0×10^{-6} (1.1×10^{-6} to 1.1×10^{-5}
WC–8%Co hard metal	2.1×10^{-6} (WC particles)[a]
Soda–lime glass	–

[a] Value obtained in the previous study [21].

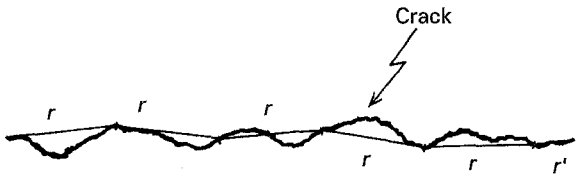

Figure 1 Approximation of a crack profile by the coarse-graining method using line segments of length r (r', a fraction of line segments).

with the length of line segments, r, through the fractal dimension, D, such that

$$N = N_0 r^{-D} \tag{3}$$

where N_0 is a constant. Therefore, the length of a crack, L, in the fractal analysis is given by

$$L = rN = N_0 r^{1-D} \tag{4}$$

However, a small fraction of line segments, r', is generally retained when one approximates the crack profile by N line segments of arbitrary length, r (Fig. 1). In this study, the length of a crack, L, is determined owing to the following condition

$$\text{if } r' \geqslant 0.5r, \text{ then } L = (N+1)r \tag{5a}$$

and

$$\text{if } r' < 0.5r, \text{ then } L = Nr \tag{5b}$$

The fractal dimension of an indentation crack, D, can be obtained by fitting the values of L and r to Equation 4.

3. Modelling of indentation cracks

Let us consider a two-dimensional (through-thickness) crack embedded in a material with the thickness, t (m), on the basis of the fractal geometry. The crack morphology is modelled as shown in Fig. 2 in this study. For simplicity, it is assumed that the initiator of a crack is a straight line of the length l (m) and the generator of a crack has a concave line with an open angle of $\pi - 2\phi$ at the first generation (Fig. 2a), although actual cracks have complicated geometry and have a fractal nature in statistical meaning. The same generator also leads to well-known Koch curve when $\phi = \pi/6$ (Fig. 2b) [30]. The modelled crack geometries in the following generations are shown in Fig. 2a. One can easily find the length of a line segment, $r^{(n)}$, and the total line length, $L^{(n)}$, at the nth generation ($n \geqslant 1$) from the geometrical consideration. At the first generation, these are given by

$$r^{(1)} = l/(2\cos\phi) \quad \text{(m)} \tag{6a}$$

$$L^{(1)} = 2r^{(1)} = l/\cos\phi \quad \text{(m)} \tag{6b}$$

where $1/(2\cos\phi) < 1$. At the second generation, $r^{(2)}$ and $L^{(2)}$ are expressed as

$$r^{(2)} = r^{(1)}/(2\cos\phi) = l/(2\cos\phi)^2 \quad \text{(m)} \tag{7a}$$

$$L^{(2)} = 2^2 r^{(2)} = l/(\cos\phi)^2 \quad \text{(m)} \tag{7b}$$

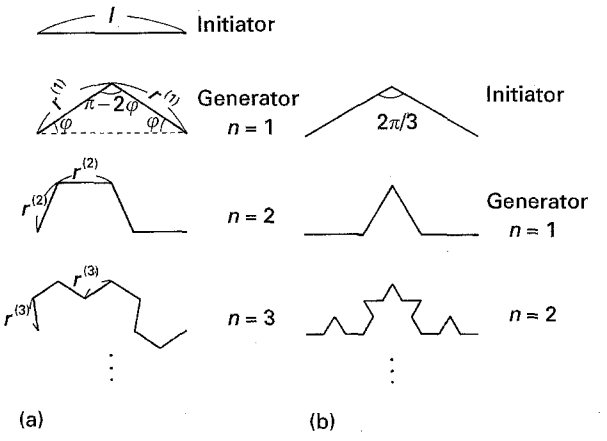

Figure 2 Schematic illustration of the modelled crack: (a) modelled crack; (b) Koch curve.

And $r^{(m)}$ and $L^{(m)}$ at the mth generation are given by

$$r^{(m)} = l/(2\cos\phi)^m \quad \text{(m)} \tag{8a}$$

$$L^{(m)} = 2^m r^{(m)} = l/(\cos\phi)^m \quad \text{(m)} \tag{8b}$$

Therefore, the fractal dimension of the modelled crack (Fig. 2a), $D(1 \leqslant D \leqslant 2)$, is expressed as

$$D = \ln 2/\ln(2\cos\phi) \tag{9}$$

and

$$\cos\phi = 2^{1/D-1} \tag{10}$$

Substituting Equation 10 into Equations 8a and b, one obtains

$$r^{(m)} = l\,2^{-m/D} \quad \text{(m)} \tag{11a}$$

$$L^{(m)} = l\,2^{m(1-1/D)} \quad \text{(m)} \tag{11b}$$

It is considered that a crack generally exhibits a fractal nature in a limited scale range between r_{min} and r_{max} ($r_{min} \leqslant r^{(m)} \leqslant r_{max}$). In this scale range, the maximum crack length, L_{max}, can be measured at the lower limit value of $r^{(m)}$, r_{min}, and the minimum crack length, L_{min}, can be estimated at the upper limit value of $r^{(m)}$, r_{max}. At the lower limit, one can find, by putting $r^{(m)} = r_{min}$ in Equation 11a, that

$$m = D\ln(l/r_{min})/\ln 2 \tag{12}$$

Substituting Equation 12 into Equation 11b, one obtains the maximum crack length, $L^{(m)} = L_{max}$, and the maximum crack surface area, S_{max}

$$L_{max} = l^D r_{min}^{-(D-1)} \quad \text{(m)} \tag{13a}$$

$$S_{max} = tL_{max} = tl^D r_{min}^{-(D-1)} \quad \text{(m)}^2 \tag{13b}$$

One can also find, by putting $r^{(m)} = r_{max}$ in Equation 11a at the upper limit, that

$$m = D\ln(l/r_{max})/\ln 2 \tag{14}$$

Substituting Equation 14 into Equation 11b, one obtains the minimum crack length, $L^{(m)} = L_{min}$, and the minimum crack surface area, S_{min}, in this scale range

$$L_{min} = l^D r_{max}^{-(D-1)} \quad \text{(m)} \tag{15a}$$

$$S_{min} = tL_{min} = tl^D r_{max}^{-(D-1)} \quad \text{(m)}^2 \tag{15b}$$

The projected crack length, $L_{min} = l$ is obtained by putting $r_{max} = l$ in Equation 15a. Let us introduce the dimensionless quantities, namely, the normalized maximum surface area of the crack, $S' = S_{max}/S_{min}$, and the normalized lower limit scale, $r_L = r_{min}/r_{max}$. The value of S' is obtained from Equation 13b and 15b, such that

$$\begin{aligned} S' &= S_{max}/S_{min} \\ &= (r_{min}/r_{max})^{-(D-1)} \\ &= r_L^{-(D-1)} \end{aligned} \quad (16)$$

Equation 16 represents a fractal nature of the crack surface.

The energy release rate due to the crack formation, g, in which the fractal nature of a crack (or a crack surface) is taken into account, is given by the following equation

$$\begin{aligned} g &= 2\Gamma S' \\ &= 2\Gamma r_L^{-(D-1)} \quad (\mathrm{J\,m^{-2}}) \end{aligned} \quad (17)$$

where Γ is the work done in creating a unit crack surface [31]. The plane strain fracture toughness, K_{IC}, is expressed by the fracture mechanics theory as

$$K_{IC} = [gE/(1 - \nu^2)]^{1/2} \ (\mathrm{MPa\,m^{1/2}}) \quad (18)$$

where E is Young's modulus and ν is Poisson's ratio. One can find from Equations 17 and 18 that

$$\begin{aligned} K_{IC} &= [2\Gamma S'E/(1 - \nu^2)]^{1/2} \\ &= [2\Gamma r_L^{-(D-1)}E/(1 - \nu^2)]^{1/2} (\mathrm{MPa\,m^{1/2}}) \end{aligned} \quad (19)$$

Therefore, the logarithmic value of K_{IC} is expressed as

$$\ln K_{IC} = 1/2\ \{(\ln[2\Gamma E/(1 - \nu^2)] - (D\text{-}1)\ \ln r_L\} \quad (20)$$

The same results of the calculation can be obtained if the crack shape was simulated to a Koch curve. Mecholsky *et al.* [9] and Milman *et al.* [10] studied fracture surfaces of alumina and glass-ceramics and fitted the relation between the fractal dimension of fracture surfaces, D', and the critical stress intensity factor, K_{IC}, with the form $K_{IC} = K_0 + Ea_0^{1/2}(D' - 1)^{1/2}$ (where K_0 is the value of K_{IC} for the hypothetical material with the smooth fracture surface and a_0 is a parameter that has unit of length). The present analysis gives a different relationship between K_{IC} and $D(D')$, as shown in Equations 19 and 20. The toughening effect arising from the fractal nature of a crack is represented in the second term $[-0.5(D - 1)\ln r_L]$ in Equation 20, where r_L is r_{min}/r_{max}, a ratio of the lower limit, r_{min}, and the upper limit, r_{max}, of the scale length, r, between which a crack exhibits a fractal nature ($r_{min} \leqslant r \leqslant r_{max}$). The value of r_{min} is assumed to be of the order of the atomic spacing in brittle materials [5] and that of r_{max} is related to the crack length or the size of microstructures such as grain diameter, whereas these values should be determined in the fractal analysis of a crack. Therefore, any discrepancy between the measured K_{IC} and the value determined from $[2\Gamma E/(1 - \nu^2)]^{1/2}$ is then due to the "fractal toughening" ($-0.5(D - 1)\ln r_L$ in Equation 20). As indicated in Equation 20, a larger fractal toughening is expected for a crack with a larger value of D in brittle materials, which has a fractal nature in a wider scale range of the fractal analysis (i.e. a smaller value of r_L), because the value of $-0.5\ln r_L$ represents the extent of fractal toughening. The value of Γ is also an important factor for the prediction of K_{IC} in a given brittle material from Equation 19 or 20, because a larger value of Γ may also lead to a larger value of K_{IC}. However, the value of Γ that should be used in the calculation is that corresponding simply to the creation of two flat surfaces without any microstructural toughening.

4. Results and discussion

4.1. Morphology of indentation cracks

Figs 3 and 4 show examples of the microstructures in the indentation-fractured specimens of brittle materials. Short indentation cracks can be seen at the corners of indentation in the specimen of WC–8%Co hard metal (Fig. 3a). The shape of the indentation cracks in the specimen of WC–8%Co hard metal seems to be straight at low magnification, but it is considerably serrated at the higher magnification (Fig. 4). The indentation cracks were principally propagated along the interface between WC particles and cobalt-binder phase or through the grain boundaries between WC particles in this specimen, while an extensive plastic deformation in the cobalt-phase was observed in the fractured SENB (single edge-notched bend) specimens of the same material [21]. The indentation cracks are short and serrated in the specimen of HP-AlN ceramics (Fig. 3b), because the cracks extended not only through the grains but also along the grain boundaries. Long and almost straight indentation cracks are visible in a large grain of SiC in the specimen of Norton NC-430 SiC ceramics (Fig. 3c), whereas short and serrated cracks were induced by indentation in the fine-grained region. Long and straight indentation cracks were also observed in the specimens of soda–lime glass.

4.2. Fractal dimension of indentation crack

Fig. 5 shows the relations between the length of the indentation crack, L, and the scale length of the fractal analysis, r, in the specimens of brittle materials. Solid symbols in the figure show the datum points which were fitted well to a single $\log_{10}L - \log_{10}r$ line and were therefore used for the estimation of the fractal dimension of the indentation crack in the indentation-fractured specimens. The fractal dimension of the crack, D, was typically estimated in the length scale range of the analysis from 2.7×10^{-7} to 1.1×10^{-5} m, and is shown in this figure. The crack length, L, decreases with increasing the scale of the analysis, r, in these specimens. The maximum value of r used for the estimation of the fractal dimension of the crack, D, is in the range from 5.5×10^{-6} to 1.1×10^{-5} m in the specimens of brittle materials. This value is about three times as much as the average diameter of WC particles (about 2.1 μm) in the specimen of WC–8%Co hard metal, and is a few times larger than or of the order of the average grain diameter in the specimens of

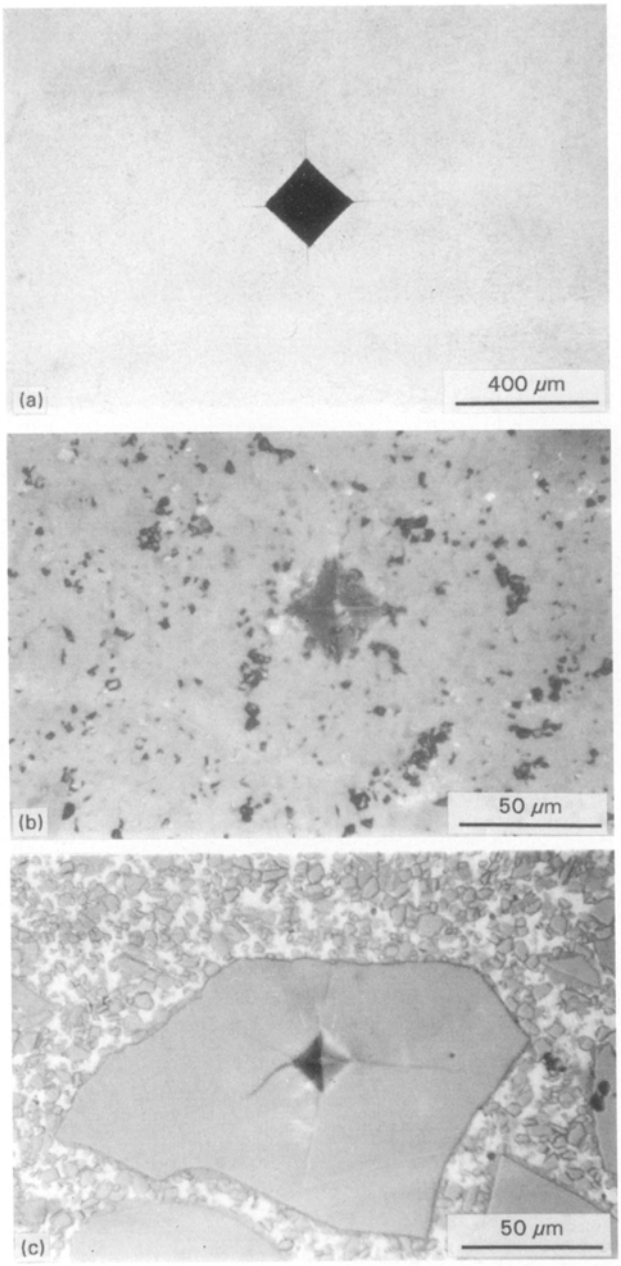

Figure 3 Examples of the microstructures in the indentation-fractured specimens of brittle materials. (a) WC–8%Co hard metal, (b) HP–AlN ceramics, (c) Norton NC-430 SiC ceramics.

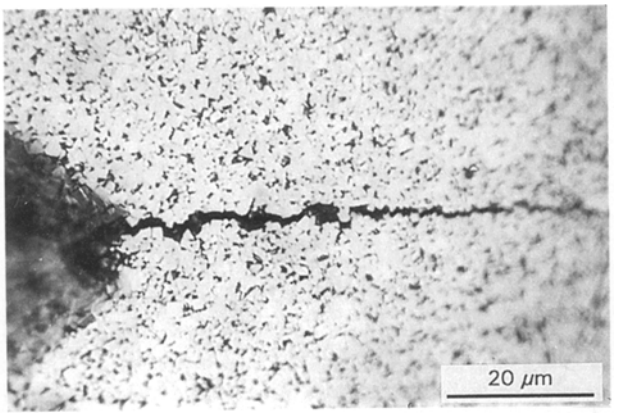

Figure 4 The optical micrograph of an indentation crack in a specimen of WC–8%Co hard metal.

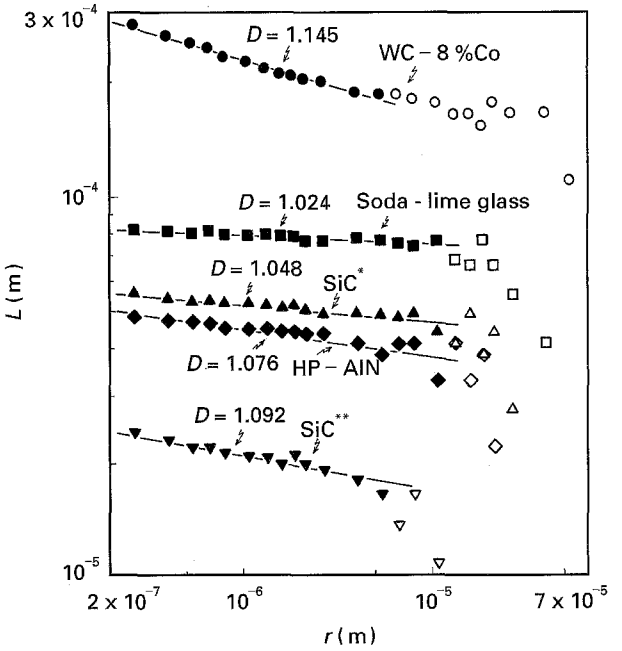

Figure 5 The relations between the length of the indentation crack, L, and the scale length of the fractal analysis, r, in the specimens of brittle materials: (*) coarse-grained region; (**) fine-grained region.

HP-AlN and Norton NC-430 SiC ceramics (Table II). The fractal dimension of the indentation crack, D, was in the range from 1.024 (soda–lime glass) to 1.145 (WC–8%Co hard metal). The data points become considerably scattered when the scale of the fractal analysis approaches the projected length of the indentation crack. For this reason, the value of the fractal dimension of the indentation crack was estimated using the data points of L corresponding to the values of r which are below about 30% of the projected crack length. Thus, the upper limit of the scale length, r_{max}, in the fractal analysis below which a crack exhibits a fractal nature, is related to the size of microstructures such as grain diameter or the indentation crack size, and is considered to be in the range of about 5×10^{-6} to about 10^{-4} m in these specimens. The value of r_{min} cannot be determined from the experimental results in this study. But, as described earlier, this value is assumed to be the order of atomic spacing in brittle materials [5].

4.3. Relationship between indentation fracture toughness and fractal dimension of crack

Table III shows the values of the indentation fracture toughness, K_c, and the fractal dimension of the indentation crack, D, in the specimens of brittle materials obtained in this study. The indentation fracture toughness increases with increasing the fractal dimension of the crack in these specimens. The K_c value (14.1 MPa $m^{1/2}$) is close to the K_{IC} value (13.3 MPa $m^{1/2}$) in the WC–8%Co hard metal obtained in the previous study [21] (Table I). The value of a soda–lime glass (0.604 MPa $m^{1/2}$) is much the same as the K_{IC} values given by Pampuch [32] (0.2–0.7 MPa $m^{1/2}$) and is close to the value $K_{IC} = 0.68$

TABLE III The values of the indentation fracture toughness, K_c, and of the fractal dimension of the indentation crack, D, in the specimens of brittle materials

Material	Indentation fracture toughness, K_c (MPa $m^{1/2}$)	Fractal dimension of indentation crack, D	Fractional part of D, $D-1$
Soda–lime glass	0.604	1.024	0.024
Norton NC-430 SiC	1.68[a]	1.048[a]	0.048[a]
	3.60[b]	1.092[b]	0.092[b]
HP-AlN	1.94	1.076	0.076
WC–8%Co hard metal	14.1	1.145	0.145

[a]Values of coarse-grained region.
[b]Values of fine-grained region.

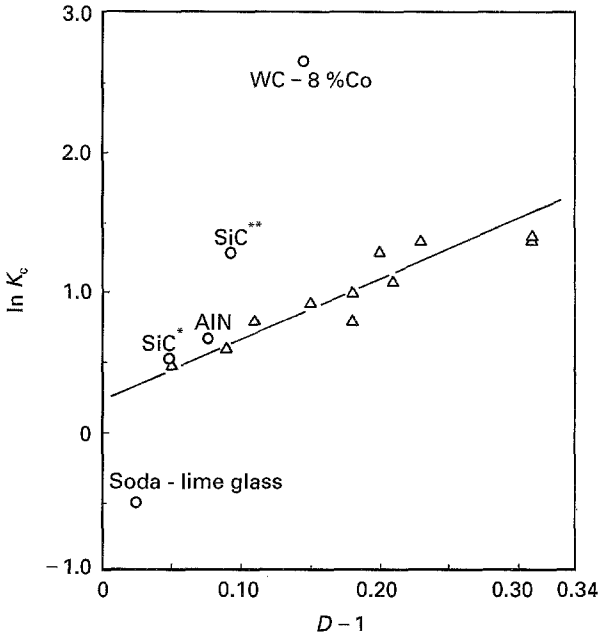

Figure 6 The relationship between the value of ln K_c and the fractional part of the fractal dimension of the crack or the fracture surface, $D-1$, in the specimens of brittle materials; (*) coarse-grained region; (**) fine-grained region. (○) Indentation crack, (△) fracture surface [9].

Mp$m^{1/2}$ calculated by using the values of $\Gamma = 1.75\ J\,m^{-2}$ and $E = 62$ GPa [33]. In Norton NC-430 SiC ceramics, the K_c value in the large grains (1.68 MPa$m^{1/2}$) is smaller than the K_{IC} value (3.5 MPa$m^{1/2}$) reported by the manufacturer (Table I), but the K_c value in the fine-grained region (3.60 MPa$m^{1/2}$) is close to this value. Unfortunately, no available data for the K_{IC} value were reported by the manufacturer on the HP-AlN ceramics.

Fig. 6 shows the relationship between the value of ln K_c and the fractional part of the fractal dimension of the crack, D–1, in brittle materials. The experimental data of the critical stress intensity factor, K_{IC}, and the fractal dimension of the fracture surface, D', on alumina and glass-ceramics obtained by Mecholsky *et al.* [9] are also shown in this figure. Their fractal data shown in this figure were estimated by the slit island method. It is assumed that both fracture surface and indentation crack surface have an identical value of fractal dimension in the same material ($D' = D$). Further, the value of r_{max}, below which the fracture surface shows a fractal nature, is considered to be less than 10^{-4} m in their alumina and glass-ceramics, because the maximum area of islands in the slit island method is less than $5 \times 10^{-9}\ m^2$ in their results. Although there is a scatter among the datum points, the relationship between the value of ln K_c and the fractal dimension, D, in brittle materials except WC–8%Co hard metal is fitted by the regression analysis to Equation 20, and is given by

$$\ln K_c = 0.218 + 4.27\,(D-1) \quad (\gamma = 0.7836) \quad (21)$$

where γ is a correlation factor. The datum points of WC–8%Co with very large value of K_c, in which the effect of plastic deformation is not negligible [21], is therefore excluded from the regression analysis. The value of $r_L = 1.9 \times 10^{-4}$ can be obtained from Equation 21. The value of r_L is a ratio of the lower limit, r_{min}, to the upper limit, r_{max}, of the scale length of the fractal analysis, r, r_{min}/r_{max}, between which the crack or the crack surface exhibits a fractal nature ($r_{min} \leqslant r \leqslant r_{max}$) . Therefore, one can estimate the value of $r_L \simeq 10^{-5}$ to 2×10^{-4} by putting $r_{min} \simeq 10^{-9}$ m and $r_{max} \simeq 5 \times 10^{-6}$ to 10^{-4} m, because the value of r_{min} is assumed to be of the order of atomic spacing and the value of r_{max} is related to the size of microstructures such as grain diameter or crack length. As described above, the value of r_{max} is considered to be less than 10^{-4} m for the fractal data of alumina and glass-ceramics [9]. The value of r_L obtained from Equation 21 (1.9×10^{-4}) is close to the upper bound value (2×10^{-4}) calculated using the values of r_{min} and r_{max}, while the value of $K_c = 1.24$ MPa$m^{1/2}$ obtained by putting $D = 0$ in Equation 21 is somewhat larger compared with the value of K_{IC} for glass (0.2–0.7 MPa$m^{1/2}$) [32]. As described in Section 3, the value of r_L represents the extent of "fractal toughening" due to the crack morphology, and a smaller value of r_L may lead to a larger toughening in brittle materials. Further, the value of Γ is also an important factor and the value that should be used in Equation 20 or 19 is that corresponding simply to the creation of two flat surfaces without any microstructural toughening. Therefore, one can predict the fracture toughness of a given brittle material, K_{IC}, from Equation 20 (or Equation 19) by using the reliable data of the fractal dimension of the crack or the fracture surface, D, and the values of r_L and Γ.

5. Conclusions

The relationship between the indentation fracture toughness, K_c, and the fractal dimension of the crack, D, were examined on the indentation-fractured specimens of SiC and AlN ceramics, a soda–lime glass and a WC–8%Co hard metal. The theoretical equation based on a fractal geometry model was developed to correlate the fractal dimension of the crack, D, with the fracture toughness, K_{IC}, in

brittle materials. The results obtained were summarized as follows.

1. The fractal dimension of the indentation crack, D, was in the range from 1.024–1.145 in the specimens of brittle materials. The indentation fracture toughness, K_c, increased with increasing the fractal dimension of the crack, D, in these specimens, although the specimen of WC–8%Co hard metal exhibited very large value of K_c because of its plasticity. The fractal dimension of the crack was typically estimated in the scale range of the fractal analysis, r, from 2.7×10^{-7} to 1.1×10^{-5} m, and the upper limit of the scale length, r_{max}, was related to the size of microstructures such as grain diameter or the crack length.

2. The analytical result of the indentation crack on the basis of the fractal geometry showed the relationship between the fracture toughness, K_{IC}, and the fractal dimension of the crack, D, such that

$$\ln K_{IC} = 1/2 \{ln[2\Gamma E/(1 - \nu^2)] - (D - 1)lnr_L\}$$

where Γ is the work done in simply creating a unit crack surface without any microstructural toughening, E is Young's modulus, ν is Poisson's ratio, and r_L is r_{min}/r_{max}, a ratio of the lower limit, r_{min}, to the upper limit of the length scale, r, in the fractal analysis, between which a crack exhibits a fractal nature ($r_{min} \leqslant r \leqslant r_{max}$). The second term in the above equation ($-0.5(D–1) \ln r_L$) represents the "fractal toughening" due to the crack morphology. The value of r_{min} is assumed to be of the order of atomic spacing in brittle materials and the value of r_{max} was related to the size of microstructures, such as grain diameter or the crack length.

3. The experimental data (except for WC–8%Co hard metal) obtained in this study and by Mecholsky *et al.* [9] fitted to the above equation, and the values of $r_L = 1.9 \times 10^{-4}$ and $K_{IC} = 1.24\ \text{MPa m}^{1/2}$ for $D = 0$ were obtained. The value of r_L was close to the upper bound of r_L calculated from the values of r_{min} and r_{max} (about 10^{-5} to 2×10^{-4}), while the value of K_{IC} for $D = 0$ was somewhat larger than the value of K_{IC} for glass. One can predict the fracture toughness of a given brittle material from the above theoretical equation by using the reliable data of the fractal dimension of the crack or the fracture surface, D, and the values of r_L and Γ.

Acknowledgements

The author thanks Toshiba Metals and Ceramics Laboratory Co. Ltd and Kobayashi Industry Co. Ltd for supplying the specimens of ceramic materials and WC–8%Co hard metals used in this study.

References

1. B. B. MANDELBROT, D. E. PASSOJA and A. J. PAULLAY, *Nature* **308** (1984) 721.
2. E. E. UNDERWOOD and K. BANERJI, *Mater. Sci. Eng.* **80** (1986) 1.
3. C. S. PANDE, L. E. RICHARDS, N. LOUAT, B. D. DEMPSEY and A. J. SCHWOEBLE, *Acta Metall.* **35** (1987) 1633.
4. K. ISHIKAWA, T. OGATA and K. NAGAI, *J. Mater. Sci. Lett.* **8** (1989) 1326.
5. S. MATSUOKA, H. SUMIYOSHI and K. ISHIKAWA, *Trans. Jpn Soc. Mech. Eng.* **56** (1990) 2091.
6. R. H. DAUSKARDT, F. HAUBENSAK and R. O. RITCHIE, *Acta Metall. Mater.* **38** (1990) 143.
7. E. HORNBOGEN, *Z. Metallkde* **78** (1987) 622.
8. M. TANAKA and H. IIZUKA, *ibid.* **82** (1991) 442.
9. J. J. MECHOLSKY, D. E. PASSOJA and K. S. FEINBERG-RINGEL, *J. Am. Ceram. Soc.* **72** (1989), 60.
10. V. Y. MILMAN, N. A. STELMASHENKO and R. BLUMENFELD, *Progr. Mater. Sci.* **38** (1994) 425.
11. W. D. KINGERY, H. K. BOWEN and D. R. UHLMANN, "Introduction to Ceramics" 2nd Edn, (J. Wiley New York, 1976) p. 796.
12. D. W. RICHERSON, "Modern Ceramic Engineering", 2nd Edn, (Marcel Dekker, New York, 1992) p. 731.
13. Z. G. WANG, D. L. CHEN, X. X. JIANG, S. H. AI and C. H. SHIH, *Scripta Metall.* **22** (1988) 827.
14. M. TANAKA, *J. Mater. Sci.* **27** (1992) 4717.
15. *Idem, Z. Metallkde* **84** (1993) 697.
16. *Idem, J. Mater. Sci.* **28** (1993) 5753.
17. T. NISHIDA and E. YASUDA, "The Evaluation of Mechanical Properties of Ceramics," (Nikkan Kogyo Shinbunsha, Tokyo, 1986) p. 63.
18. K. NIIHARA, R. MORENA and D. P. H. HASSELMAN, in "Fracture Mechanics of Ceramics", Vol. 5, edited by R. C. Bradt, A. G. Evans, D. P. H. Hasselman and F. F. Lange (Plenum Press, New York, London, 1983) p. 97.
19. Z. LI, A. GHOSH, A. S. KOBAYASHI and R. C. BRADT, *J. Am. Ceram. Soc.* **74** (1991) 889.
20. S. SRINIVASAN and R. O. SCATTERGOOD, *ibid.* **74** (1991) 887.
21. H. IIZUKA and M. TANAKA, *J. Mater. Sci.* **26** (1991) 4394.
22. A. KELLY, "Strong Solids," translated by Y. Murakami, (Maruzen, Tokyo, 1971) p. 221.
23. A. MURAMATSU, "Elastic Moduli of Metallic Materials," (Japan Society of Mechanical Engineers, Tokyo, 1980) p. 227.
24. G. PETZOW, "Metallographisches Ätzen," translated by G. Matsumura (AGNE, Tokyo) p. 56.
25. R. L. FULLMAN, *Trans. AIME* **197** (1953) 447.
26. B. R. LAWN, A. G. EVANS and D. B. MARSHALL, *J. Am. Ceram. Soc.* **63** (1980) 574.
27. K. NIIHARA, R. MORENA and D. P. H. HASSELMAN, *J. Mater. Sci. Lett.* **1** (1982) 13.
28. H. TAKAYASU, "Fractals in the Physical Sciences" (Manchester University Press, Manchester, New York, 1990) p. 11.
29. S. ISHIMURA and S. ISHIMURA, "Fractal Mathematics" (Tokyo Book Co., Tokyo, 1990) p. 240.
30. B. B. MANDELBROT, "The Fractal Geometry of Nature," translated by H. Hironaka (Nikkei Science, Tokyo, 1989) p. 42.
31. R. W. DAVIDGE, "Mechanical Behaviour of Ceramics," translated by H. Suzuki and T. Iseki (Kyoritsu, Tokyo, 1982), p. 35.
32. R. PAMPUCH, "Constitution and Properties of Ceramic Materials" (Elsevier, Amsterdam, 1991) p. 68.
33. B. R. LAWN, "Fracture of Brittle Solids" 2nd Edn (Cambridge University Press, Cambridge, 1993) p. 9.

Received 17 June 1994
and accepted 17 July 1995